Electrokinetic Preconcentration and Detection of Neuropeptides at Patterned Graphene-Modified Electrodes in a Nanochannel

ARTICLE *in* ANALYTICAL CHEMISTRY · APRIL 2014

Impact Factor: 5.64 · DOI: 10.1021/ac500155g · Source: PubMed

5 AUTHORS, INCLUDING:

Bankim Sanghavi
University of Virginia
17 PUBLICATIONS **976** CITATIONS
SEE PROFILE

Walter Varhue
University of Virginia
12 PUBLICATIONS **92** CITATIONS
SEE PROFILE

Nathan Swami
University of Virginia
88 PUBLICATIONS **971** CITATIONS
SEE PROFILE

analytical chemistry

Letter

pubs.acs.org/ac

Electrokinetic Preconcentration and Detection of Neuropeptides at Patterned Graphene-Modified Electrodes in a Nanochannel

Bankim J. Sanghavi,[†] Walter Varhue,[†] Jorge L. Chávez,[‡] Chia-Fu Chou,[§] and Nathan S. Swami*[,†]

[†]Department of Electrical and Computer Engineering, University of Virginia, Charlottesville, Virginia 22904, United States

[‡]Human Effectiveness Directorate, 711th Human Performance Wing, Air Force Research Laboratory, Dayton, Ohio 45433, United States

[§]Institute of Physics, Academia Sinica, Taipei 11529, Taiwan

Supporting Information

ABSTRACT: Neuropeptides are vital to the transmission and modulation of neurological signals, with Neuropeptide Y (NPY) and Orexin A (OXA) offering diagnostic information on stress, depression, and neurotrauma. NPY is an especially significant biomarker, since it can be noninvasively collected from sweat, but its detection has been limited by poor sensitivity, long assay times, and the inability to scale-down sample volumes. Herein, we apply electrokinetic preconcentration of the neuropeptide onto patterned graphene-modified electrodes in a nanochannel by frequency-selective dielectrophoresis for 10 s or by electrochemical adsorptive accumulation for 300 s, to enable the electrochemical detection of NPY and OXA at picomolar levels from subnanoliter samples, with sufficient signal sensitivity to avoid interferences from high levels of dopamine and ascorbic acid within biological matrices. Given the high sensitivity of the methodology within small volume samples, we envision its utility toward off-line detection from droplets collected by microdialysis for the eventual measurement of neuropeptides at high spatial and temporal resolutions.

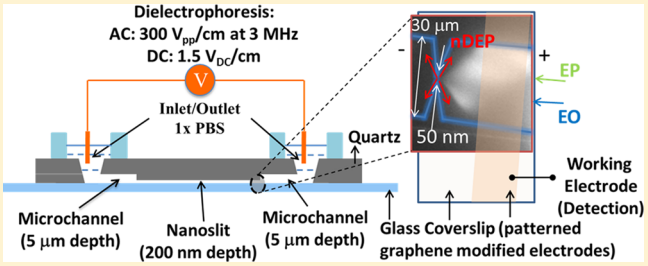

Neuropeptides form a significant class of neurotransmitters and neuromodulators.[1] Their sensitive measurement at high spatial and temporal resolution offers information on the chemistry, biology, and pharmacology of the nervous system. However, their presence, at picomolar levels within the brain[2] and at even lower levels within sweat,[3] poses analytical challenges due to interferences from other biomolecules at far higher levels. This is accentuated by the low recovery of neuropeptides by microdialysis (<20%), the small volume of the generated dialysate, and the difficulties associated with sample storage.[4] Neuropeptide Y (NPY), the most abundant of the neuropeptides, can be collected in a noninvasive manner from sweat by using a skin patch. It is a biomarker for stress and depression[5] that is of interest for the diagnosis of post-traumatic stress disorder (PTSD), traumatic brain injury, and neuro-trauma.[6] Other neuropeptides of interest include the C-terminal fragment of NPY (NPY 18-36), which is applied as an antagonist of NPY function, and Orexin A (OXA), which offers information on arousal, wakefulness, and appetite.

The measurement of NPY has been carried out previously by mass spectrometry following chromatographic separation (HPLC-MS) from plasma samples.[7] However, the sensitivities are not sufficient for diagnostic information, and scale-down of sample volume is challenging. Immunoassays, following microdialysis from brain[2] and sweat samples,[8] have picomolar level detection limits. However, their quantification is hindered by cross-reactivity with other peptides in the matrix, which are usually present at far higher levels than NPY. Additionally, since immunoassays involve multiple incubation steps, they are not suited for continuous monitoring. Electrochemical detection is widely applied for the ultrafast measurement of neurotransmitters, following separation by capillary electrophoresis (CE-EC),[9] but poor sensitivities have been reported for NPY.[10] Electrochemical sensitivities on glassy carbon electrodes (GCEs) can be enhanced by nanomaterial modifiers,[11] to lower background current and enhance analyte adsorption kinetics.[12] However, at subnanomolar levels, the detection sensitivity is limited by analyte transport to the sensing region rather than by signal sensitivity at the electrode. Hence, in addition to electrode modification, there is a need to enhance flux toward the sensor by selective preconcentration of the analyte, especially within microfluidic or nanochannel device platforms[13] that enhance adsorption due to short diffusion lengths and high surface to volume ratios.

Herein, we report on the electrochemical measurement of neuropeptides at picomolar levels from subnanoliter sample volumes by enabling electrokinetic preconcentration of the neuropeptide onto graphene-modified electrodes that are patterned in a nanochannel device to enhance electrochemical detection sensitivity, by providing a high conductivity surface

Received: January 7, 2014
Accepted: April 4, 2014
Published: April 4, 2014

   dx.doi.org/10.1021/ac500155g | *Anal. Chem.* 2014, 86, 4120−4125

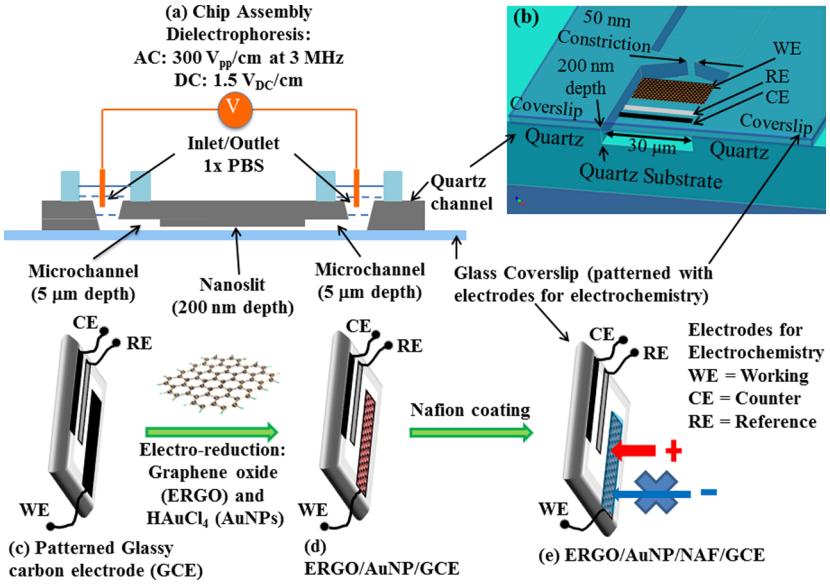

Figure 1. Cross-section (a) and top-view (b) of the chip assembly with microchannel reservoirs (5 μm depth) and slit shaped nanochannels (200 nm depth) containing ~50 nm lateral constrictions fabricated on a quartz substrate and bonded to a glass coverslip with patterned electrochemical electrodes, including graphene-modified working electrode (fabricated as per: (c)–(e)), Ag/AgCl reference electrode, and counter electrode that are aligned orthogonally to fit in the nanochannel in proximity of the lateral constriction.

with fast adsorption kinetics. Localized analyte preconcentration under physiological conditions is accomplished by either: (a) electrochemical adsorptive accumulation or (b) frequency-selective negative dielectrophoretic (nDEP) trapping of NPY. In prior work, we have applied DEP techniques within physiological media to cause preconcentration of single-stranded DNA within microfluidic channels[14] for enhancing DNA hybridization kinetics[15,16] and enabling million-fold enrichment of proteomic biomarkers at nanochannel constrictions within a few seconds.[17−19] In the current work, by integrating DEP enrichment to electrochemical detection on high-conductivity graphene-modified electrodes in a nanochannel, we demonstrate the detection of highly relevant neuropeptide biomarkers at sensitivities comparable to immunoassays, but at far more rapid assay times and with far less sample volumes. Given the high sensitivity of the methodology within subnanoliter samples, we envision its utility toward off-line detection from droplets collected by microdialysis at varying locations or time points from tissues, for the eventual measurement of neuropeptides at high spatial and temporal resolutions.[20]

METHODS

The microfluidic chip, utilizing ~0.1 nL sample volume, consists of a quartz substrate nanofabricated with the channel structures[17,18] and bonded to a glass coverslip that is microfabricated with electrochemical working, counter, and reference electrodes (Figure 1). As per the cross-sectional view in Figure 1a, the chip includes an inlet and outlet leading to microchannel reservoirs (5 μm depth and 750 μm width) and several slit-shaped nanochannels (200 nm depth) that contain lateral constrictions (30 μm down to 50 nm in width), arranged ~100 μm from the interface of the nanochannel to the microchannel (Figure 1b). Electrochemical detection electrodes (30 μm width for coupling to nDEP) are fabricated on coverslip glass (Figure 1c–e), by converting the patterned resist to glassy carbon (GCE) by standard pyrolysis methods,[21] followed by electro-reduction of graphene oxide (ERGO),[22] electrodeposition of AuNPs at −0.8 V for 60 s in 1 mM $HAuCl_4$, and the drop casting of Nafion (NAF) under a stereomicroscope. Alternate patterned electrodes on the coverslip function as counter and reference electrodes for electrochemistry. The Ag/AgCl reference is prepared by electrodeposition with Ag and treatment with $FeCl_3$ for chloridizing the surface layer.[23] This coverslip is bonded to the nanoslit quartz substrate,[24] after ensuring that the length-edge of the graphene-modified working electrode is orthogonally aligned to be within ~1 μm from the constriction tip, to enable preconcentration in the proximity of the electrodes by negative DEP (nDEP). This device geometry ensures that the counter and reference electrodes are in the same nanochannel as the working electrode, thereby ensuring sensitive current measurement and that all potential drop occurs at the surface of the working electrode rather than in the solution. The negative DEP behavior of NPY under an AC field of 300 V_{pp}/cm at 3 MHz frequency is driven by external Pt electrodes (at inlet and outlet) using a standard function generator (Agilent 3220) and voltage amplifier (FLC), with an additional DC field of 1.5 V/cm to enhance transport of NPY toward the constriction. The preconcentration profile is optimized by observation of fluorescently labeled NPY (Phoenix) under inverted microscopy (Zeiss, Z1) using an EMCCD (Hamamatsu). Following optimization, electrochemical analysis by differential pulse voltammetry (DPV) is carried out (Solartron) using the patterned graphene-modified electrodes. For preconcentration of NPY, NPY 18-36, and OXA by electrochemical adsorptive accumulation, −0.7 V is applied to the graphene-modified electrode (10 to 450 s), followed by DPV from +0.4 to +1.0 V, using a step potential of 5 mV and modulation amplitude of 50 mV. For cyclic voltammetry (CV), the potential is scanned from 0.3 to +0.9 V. Double potential step chronocoulometry is carried out with a pulse period of 5 s from +0.45 to +0.95 V vs. Ag/AgCl. Further information on the chemicals and experimental procedures is in Section S-1 (Supporting Information). On the basis of the amino acid sequences of NPY, NPY 18-36, and OXA in Scheme S-1 and Table S-1 (Supporting

dx.doi.org/10.1021/ac500155g | Anal. Chem. 2014, 86, 4120−4125

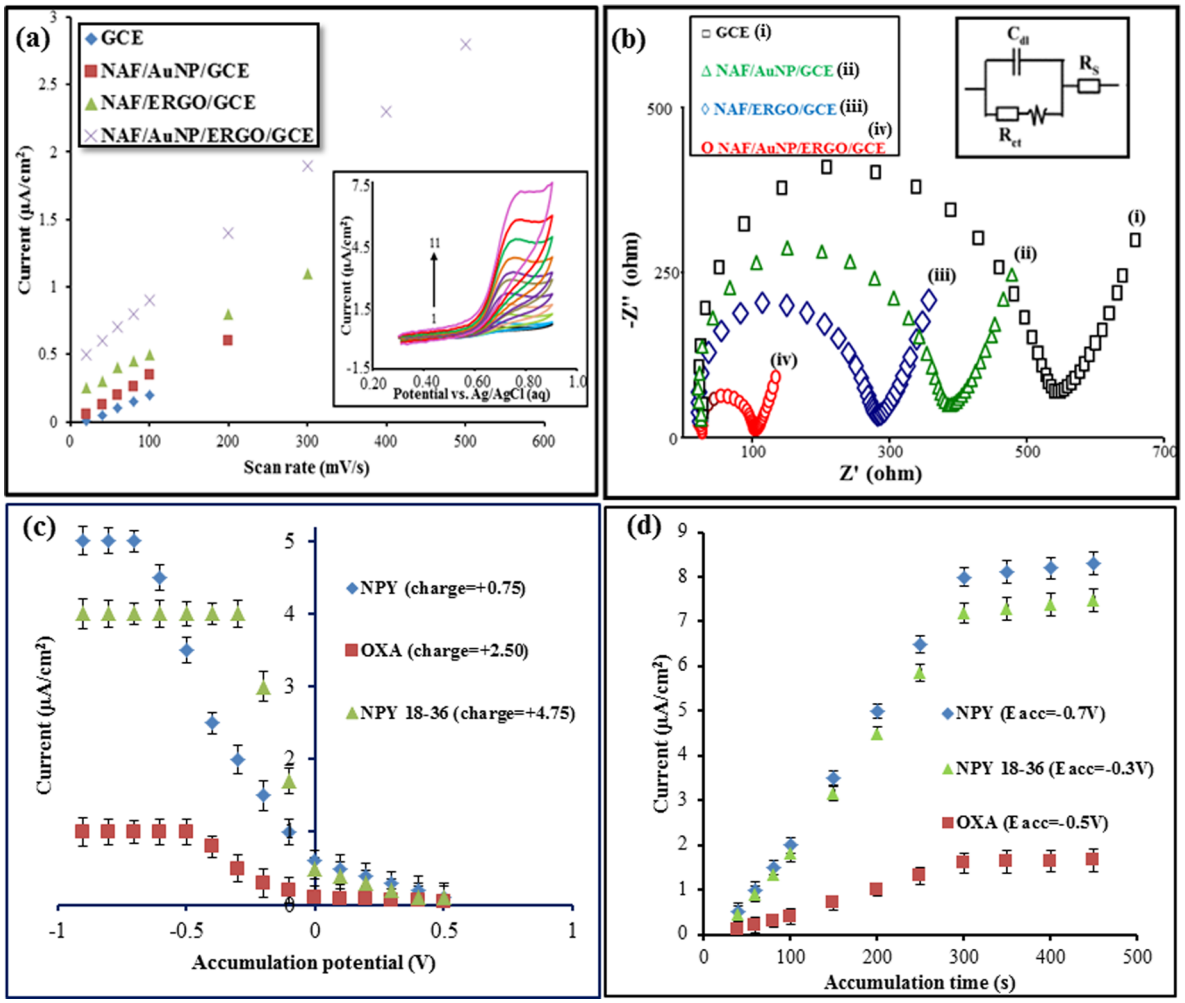

Figure 2. Optimizing graphene-modification: (a) for enhanced adsorption rate, by optimizing peak signal (1.02×10^{-8} M NPY) with varying CV scan rate (10−500 mV s^{-1}) and (b) for enhanced electron transfer rate, by optimizing electrode impedance (1 mM $[Fe(CN)_6]^{3-/4-}$) at (i) GCE; (ii) NAF/AuNP/GCE; (iii) NAF/ERGO/GCE; and (iv) NAF/ERGO/AuNP/GCE surfaces. (c) Optimizing electrochemical accumulation voltage for the neuropeptides based on their respective charge, so that peak electrochemical oxidation signal can be obtained at 300 s accumulation time (d). Note that the impedance measurements in (b) were conducted using an electrode patterned across the entire nanochannel area of ∼0.01 cm^2.

Information), electrochemical oxidation of the tyrosine moiety involves five electrons for NPY, four electrons for NPY 18-36, and one electron for OXA:

$$\text{NPY: reduced (Tyr−R−Tyr−Tyr−R−Tyr−R−Tyr)} \xrightarrow{-5e^- - 5H^+} \text{NPY: oxidized} \quad (1)$$

$$\text{NPY 18-36: reduced (R−Tyr−Tyr−R−Tyr−R−Tyr)} \xrightarrow{-4e^- - 4H^+} \text{NPY 18-36: oxidized} \quad (2)$$

$$\text{OXA: reduced (Tyr−R−Tyr)} \xrightarrow{-1e^- - 1H^+} \text{OXA: oxidized} \quad (3)$$

As per Figures S-1 and S-2 (Supporting Information), a supporting electrolyte of 0.1 M phosphate buffer at pH 6.0 leads to optimal electrochemical oxidation of NPY, as judged by the DPV peak current. The potential for electrochemical accumulation is optimized on the basis of neuropeptide charge, determined from the difference of the pH to pK_a for each of the positive and negatively charged amino acids in the respective peptide[25] (eq (S1), Supporting Information). At pH 6 in PBS electrolyte, the accumulation potential is −0.7 V for NPY due to its net charge of "+0.75", whereas a lower potential of −0.5 V is sufficient for OXA due to its higher net charge of "+2.5" and just −0.3 V is sufficient for the accumulation of NPY 18-36 due to its net charge of "+4.75" (details in Table S-1, Supporting Information, and Figure 2c,d). The NAF cation exchange overlayer on the graphene-modified electrode enables the exchange of H^+ from NAF with the NPY^+ (or OXA^+) diffusing from the bulk electrolyte.

RESULTS AND DISCUSSION

Surface modification of the patterned glassy carbon electrode is optimized for enabling analyte adsorption under preconcentration by DEP or electrochemical accumulation. Figure 2a shows the CV at scan rates of 10 to 500 mV/s (inset) with the respective peak signals from electrochemical oxidation of NPY on glassy carbon electrode [GCE: (i)], nafion and AuNP modified GCE [NAF/AuNP/GCE: (ii)], nafion and electrochemically reduced graphene oxide modified GCE [NAF/ERGO/GCE: (iii)], and finally nafion and electrochemically reduced graphene oxide and AuNP modified GCE [NAF/AuNP/ERGO/GCE: (iv)]. On the basis of the linear rise in CV signal with scan rate, we infer an adsorption rate controlled

dx.doi.org/10.1021/ac500155g | Anal. Chem. 2014, 86, 4120−4125

electron transfer process. Furthermore, since slope of the linear region is the highest for NAF/AuNP/ERGO/GCE modification (iv), we infer that this modification is most effective in enabling an analyte adsorption rate at the electrode that keeps up with its diffusional transport toward the electrode. For this NAF/AuNP/ERGO/GCE surface modification, enhancement of the electro-active surface area is confirmed by CV and the higher electrode reaction rate constant (k_s) for a constant charge transfer coefficient (α) is confirmed by the Laviron's eq (Section S-5, Supporting Information). Nyquist plots from electrochemical impedance spectroscopy (EIS) of $[Fe(CN)_6]^{3-/4-}$ (1 mM) at each of the respective GCE modified surfaces were conducted with the electrode patterned across the entire nanochannel area of ~0.01 cm^2, for optimizing the surface modification for enhanced electron transfer. Figure 2b shows that the charge transfer resistance (R_{ct}) values exhibit a decrease from 510.12 Ω at GCE to 370.24 Ω at NAF/AuNP/GCE, 250.21 Ω at NAF/ERGO/GCE, and 90.16 Ω at NAF/AuNP/ERGO/GCE. The enhanced adsorption and electron-transfer kinetics due to the NAF/AuNP/ERGO/GCE modification is confirmed to result in the highest DPV signals for NPY (Figure S-3, Supporting Information). XRD and UV−vis characterization of this modified electrode are shown in Section S-6 (Figures S-4 and S-5), Supporting Information. Figure 2c confirms that the negative potential required for optimal electrochemical accumulation increases with decreasing positive charge on the neuropeptide, while Figure 2d shows that optimal accumulation under these potential conditions can be obtained within 300 s for each of the three neuropeptides.

The dielectrophoretic preconcentration of NPY (300 V_{pp}/cm at 3 MHz with 1.5 V_{DC}/cm) occurs away from the high field points at the lateral constrictions within the nanochannel (Figure 3). In prior work, we have utilized the frequency selective characteristics of dielectrophoresis to preconcentrate streptavidin by positive DEP (pDEP) in the 30−200 kHz range and by nDEP in the 1 MHz range,[17] as well as to separate streptavidin from goat antihuman IgG (Ga−H IgG) based on differences in the preconcentration rate at 1 MHz.[18] Herein, we choose a 3 MHz frequency, since nDEP trapping continues to be significant for NPY, while other interfering biomolecules, such as streptavidin and IgG, do not show significant dielectrophoresis behavior at this high frequency. As per the fluorescence images in Figure 3a−f, it is apparent that NPY molecules are preconcentrated away from the constriction tip and onward over an extent of ~100 μm until the interface of the nanochannel to the adjoining microchannel. The electrokinetic force balance of Figure 3g explains the preconcentration profile in terms of the force balance of electrophoresis (EP) and electro-osmosis (EO) on one side versus nDEP on the other side, with nDEP being dominant only in the localized region adjoining the gradient caused by the constriction, due to its ∇E^2 dependence, whereas EO and EP are less localized due to their linear dependence on the field (E). Within the assembled microfluidic device, the graphene-modified detection electrodes are aligned to fit on top of this DEP preconcentration region. Next, we compare the detection accomplished by preconcentration of NPY through adsorptive accumulation under a negative potential of −0.7 V versus that by DEP. As per Figure 4a,b, the signal level after adsorptive accumulation for 300 s could be reached within 10 s of DEP preconcentration at both 10 nM and 10 pM levels of NPY. Since ascorbic acid (AA, pK_a = 4.17) and uric acid (UA, pK_a = 5.7) exist in anionic form at pH 6.0 PBS, they are not adsorbed on NAF (a cation

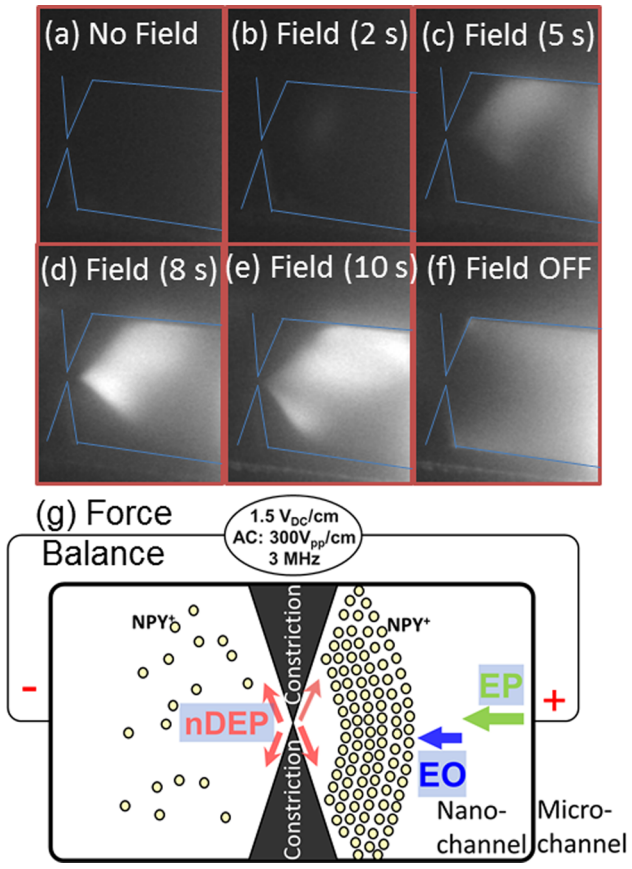

Figure 3. Preconcentration of fluorescently labeled NPY by negative dielectrophoresis (nDEP) under an AC field of 300 V_{pp}/cm at 3 MHz coupled to a DC field of 1.5 V/cm to enhance electrokinetic transport of NPY to the constriction from the microchannel reservoir.

exchanger), especially within the 10 s required for dielectrophoretic preconcentration and detection of NPY at 32 pM, as apparent from the interference studies at 1 μM ascorbic acid in Figure 4c. Since dopamine and NPY are positively charged in the pH 6 PBS buffer and since dopamine is much smaller than NPY, electrostatics under electrochemical accumulation causes dopamine peaks to dominate within interference studies of 100 nM dopamine with 32 pM NPY. However, under dielectrophoresis, the cube-fold dependence of the trapping force on size ensures that only the larger NPY molecules are trapped, whereas the much smaller dopamine molecules can only get to the electrode by free diffusion. As per the interference studies in Figure 4c with 100 nM dopamine and 32 pM NPY, based on the comparable electrochemical signals for dopamine and NPY, we estimate that DEP is able to cause ~3000-fold preconcentration within 10 s. Figure 4d shows that, while adsorptive accumulation for 100 s causes a wide linear region for signal versus analyte concentration, accumulation for 300 s causes a sharper rise of signal level with analyte concentration, thereby reaching the signal sensitivity level of 0.07 μA/cm^2 at a lower concentration value (Figure 4e). As a result, NPY can be detected down to 4 pM levels, whereas a similar analysis in Figure 4f shows detection limits of 10 pM for NPY 18-36 and 22 pM for OXA (Table S-3, Supporting Information). To substantiate that the signal at the sensitivity level of 0.07 μA/cm^2 (~700 fA on 10^{-5} cm^2 electrodes coupled to nDEP) is greater than three times that of the background for characterizing limit of detection,[26] we show the voltammograms in

dx.doi.org/10.1021/ac500155g | Anal. Chem. 2014, 86, 4120−4125

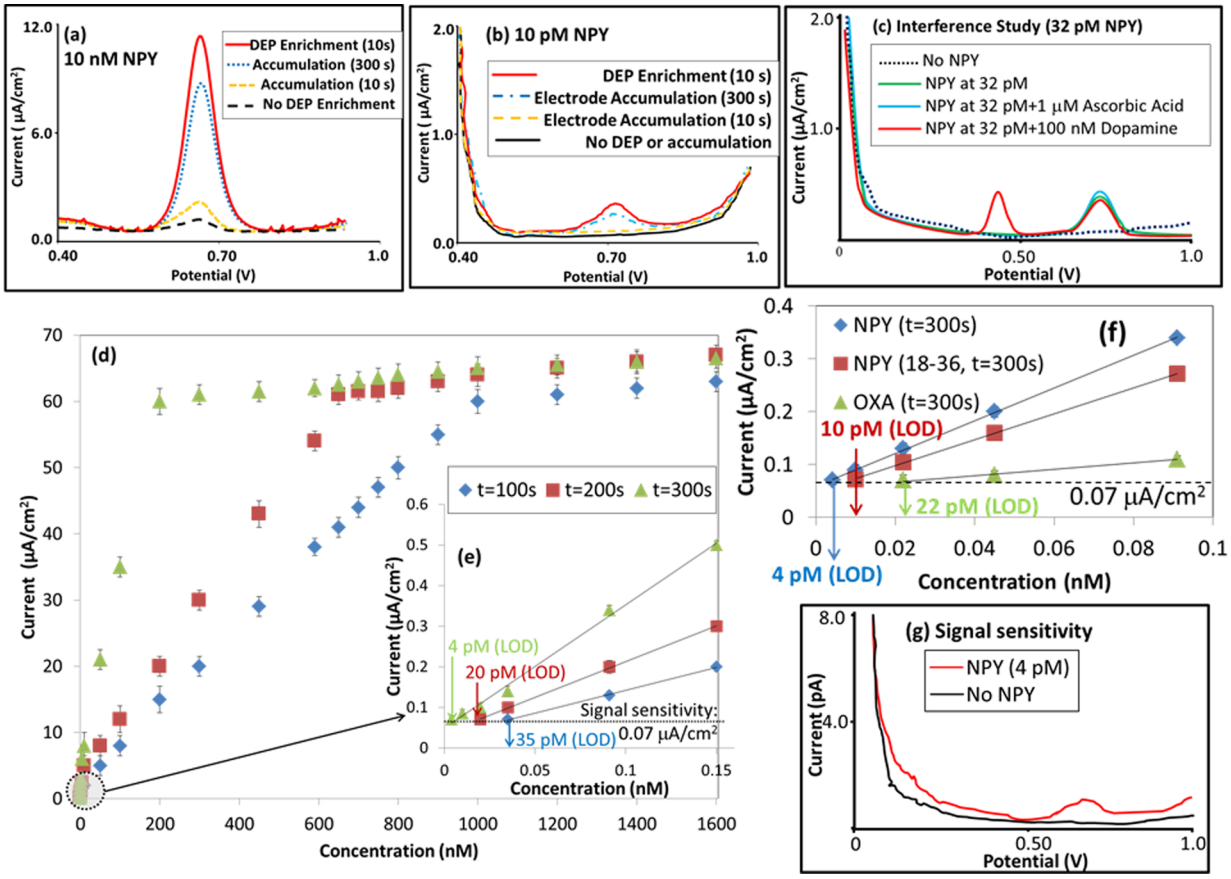

Figure 4. Signal enhancement after preconcentration by DEP versus electrochemical accumulation for various times: (a) 10 nM and (b) 10 pM NPY. (c) Interference of 100 nM dopamine and 1 μM ascorbic acid on the signal of 32 pM NPY. (d) and (e) Enhancing limit of detection (LOD) for NPY to 4 pM (300 s accumulation). (f): LOD for NPY, NPY 18-36, and OXA (300 s accumulation). (g) Voltammogram at LOD for NPY (4 pM) after 10 s of DEP preconcentration on graphene-modified electrode of 10^{-5} cm^2 area versus background (no NPY).

Table 1. Comparison of the Reported Method with the HPLC-MS Method for Neuropeptide Analysis

	NPY (10^{-9} M)		NPY 18-36 (10^{-9} M)		OXA (10^{-9} M)	
sample[c]	a[a]	b[b]	a[a]	b[b]	a[a]	b[b]
cerebrospinal fluid	2.05 ± 0.39	2.01 ± 0.61	3.25 ± 0.80	3.12 ± 0.98	4.55 ± 0.63	4.39 ± 0.77
sweat	2.11 ± 0.55	2.07 ± 0.91	3.34 ± 0.74	3.25 ± 0.90	4.49 ± 0.55	4.45 ± 0.72
saliva	2.13 ± 0.89	2.45 ± 1.34	3.28 ± 1.36	3.15 ± 1.56	4.52 ± 1.27	4.35 ± 1.56
human serum 1	2.12 ± 1.33	2.02 ± 1.52	3.29 ± 0.81	3.17 ± 1.06	4.47 ± 0.64	4.41 ± 1.02
human serum 2	2.08 ± 0.73	2.15 ± 1.11	3.34 ± 1.03	3.27 ± 1.12	4.51 ± 0.92	4.39 ± 1.41

[a]a: amount of neuropeptides (NPY/NPY 18-36/OXA) obtained by the reported method ± % RSD (n = 5). [b]b: amount of neuropeptides (NPY/NPY 18-36/OXA) obtained by the HPLC-MS method ± % RSD (n = 5). [c]Final concentration (after spiking the neuropeptide) is 2.15×10^{-9}, 3.4×10^{-9}, and 4.6×10^{-9} M for NPY, NPY18-36, and Orexin, respectively.

Figure 4g. Validation studies in Table 1 show that the reported detection platform compares well with the HPLC-MS method for quantification of the neuropeptides at nanomolar levels in cerebrospinal fluid, sweat, saliva, and blood serum samples. Recovery studies are reported in the Supporting Information (Tables S-5−S-7), and other validation studies on the detection platform are described in Tables S-3 and S-4, Supporting Information.

CONCLUSION

We present a microfluidic device methodology to couple the electrokinetic preconcentration of Neuropeptide Y (NPY) and Orexin A (OXA) with detection through electrochemical oxidation of their tyrosine moiety on high-conductivity graphene-modified electrodes in a nanochannel that were optimized for fast adsorption kinetics. NPY preconcentration was initiated by applying −0.7 V on the detection electrode for an accumulation period of 300 s or by negative dielectrophoresis for 10 s (300 V_{pp}/cm at 3 MHz with 1.5 V_{DC}/cm) for trapping away from lateral insulator constrictions and onto graphene-modified electrodes within the nanochannel. Under these conditions, NPY was detected from subnanoliter sample volumes at sensitivity levels down to 4 pM and down to 22 pM for OXA. We envision that this detection platform can be applied in conjunction with microchip capillary electrophoresis separation toward the detection of neuropeptides at high sensitivity levels and within small sample volumes for enabling measurements at high spatial and temporal resolutions.

dx.doi.org/10.1021/ac500155g | Anal. Chem. 2014, 86, 4120−4125

■ ASSOCIATED CONTENT

Supporting Information

Details on the chemicals, experimental procedures, optimization parameters, materials characterization, and sensor validation. This material is available free of charge via the Internet at http://pubs.acs.org.

■ AUTHOR INFORMATION

Corresponding Author

*Fax: +1-434-924-8818. E-mail: nswami@virginia.edu.

Notes

The authors declare no competing financial interest.

■ ACKNOWLEDGMENTS

Support was from AOARD Grants Nos. 114083 and FA2386-12-1-4002, NSF EAPSI program, and the National Science Council, Taiwan (102-2112-M-001-005-MY3). We thank Dr. Kuo-Tang Liao for assistance on nanofabrication and Dr. Nancy Kelley-Loughnane and Dr. Joshua A. Hagen of the Air Force Research Laboratory for valuable discussions.

■ REFERENCES

(1) Malva, J. O.; Xapelli, S.; Baptista, S.; Valero, J.; Agasse, F.; Ferreira, R.; Silva, A. P. *Neuropeptides* **2012**, *46*, 299−308.

(2) Gruber, S. H. M.; Nomikos, G. G.; Mathé, A. A. *Eur. Neuropsychopharmacol.* **2006**, *16*, 592−600.

(3) Cizza, G.; Marques, A. H.; Eskandari, F.; Christie, I. C.; Torvik, S.; Silverman, M. N.; Phillips, T. M.; Sternberg, E. M. *Biol. Psychiatry* **2008**, *64*, 907−911.

(4) Perry, M.; Li, Q.; Kennedy, R. T. *Anal. Chim. Acta* **2009**, *653*, 1−22.

(5) Heilig, M.; Zachrisson, O.; Thorsell, A.; Ehnvall, A.; Mottagui-Tabar, S.; Sjogren, M.; Asverg, M.; Ekmann, R.; Wahlestedt, C.; Agren, H. *J. Psychiatr. Res.* **2004**, *38*, 113−121.

(6) Andrews, J. A.; Neises, K. D. *J. Neurochem.* **2012**, *120*, 26−36.

(7) (a) Racaityte, K.; Lutz, E. S. M.; Unger, K. K.; Lubda, D.; Boos, K. S. *J. Chromatogr., A* **2000**, *890*, 135−144. (b) Rappel, C.; Schaumloffel, D. *Anal. Chem.* **2009**, *81*, 385−393. (c) Li, Q.; Zubieta, J. K.; Kennedy, R. T. *Anal. Chem.* **2009**, *81*, 2242−2250.

(8) Jia, M.; Belyavskaya, E.; Deuster, P.; Sternberg, E. M. *Anal. Chem.* **2012**, *84*, 6508−6514.

(9) Venton, B. J.; Wightman, M. R. *Anal. Chem.* **2003**, *75*, 414−421.

(10) Crespi, F. *Brain Res.* **2011**, *1407*, 27−37.

(11) Sanghavi, B. J.; Srivastava, A. K. *Electrochim. Acta* **2010**, *55*, 8638−8648.

(12) Sanghavi, B. J.; Sitaula, S.; Griep, M. H.; Karna, S. P.; Ali, M. F.; Swami, N. S. *Anal. Chem.* **2013**, *82*, 8158−8165.

(13) Schoch, R. B.; Cheow, L. F.; Han, J. *Nano Lett.* **2007**, *7*, 3895−3900.

(14) Chaurey, V.; Polanco, C.; Chou, C. F.; Swami, N. S. *Biomicrofluidics* **2012**, *6*, 012806.

(15) Swami, N. S.; Chou, C. F.; Ramamurthy, V.; Chaurey, V. *Lab Chip* **2009**, *9*, 3212−3220.

(16) Swami, N. S.; Chou, C. F.; Terbrueggen, R. *Langmuir* **2005**, *21*, 1937−1941.

(17) Liao, K. T.; Tsegaye, M.; Chaurey, V.; Chou, C. F.; Swami, N. S. *Electrophoresis* **2012**, *33*, 1958−1966.

(18) Liao, K. T.; Chou, C. F. *J. Am. Chem. Soc.* **2012**, *134*, 8742−8745.

(19) Chaurey, V.; Rohani, A.; Su, Y.-H.; Varhue, W.; Liao, K. T.; Chou, C. F.; Swami, N. S. *Electrophoresis* **2013**, *34*, 1097−1104.

(20) Nie, J.; Kennedy, R. T. *Anal. Chem.* **2010**, *82*, 7852−7856.

(21) Hebert, N. E.; Snyder, B.; McCreery, R. L.; Kuhr, W. G.; Brazill, S. A. *Anal. Chem.* **2003**, *75*, 4265−4271.

(22) Li, S.-J.; Deng, D.-H.; Shi, Q.; Liu, S.-R. *Microchim. Acta* **2012**, *177*, 325−331.

(23) Polk, B. J.; Stelzenmuller, A.; Mijares, G.; MacCrehan, W.; Gaitan, M. *Sens. Actuators, B* **2006**, *114*, 239−247.

(24) Leïchlé, T.; Lin, Y. L.; Chiang, P. C.; Liao, K. T.; Hu, S. M.; Chou, C. F. *Sens. Actuators, B* **2012**, *161*, 805−810.

(25) Moore, D. S. *Biochem. Educ.* **1985**, *13*, 10−11.

(26) *ICH Harmonised Tripartite Guideline: Validation of Analytical Procedures Methodology, International Conference on Harmonization*, 1996; http://www.ich.org/fileadmin/Public_Web_Site/ICH_Products/Guidelines/Quality/Q2_R1/Step4/Q2_R1__Guideline.pdf.